Kitaev-Heisenberg cobaltates : Coulomb exchange as leading nearest-neighbor interaction mechanism

Pritam Bhattacharyya,[1] Thorben Petersen,[1] Satoshi Nishimoto,[1,2] and Liviu Hozoi[1]

[1] *Institute for Theoretical Solid State Physics, Leibniz IFW Dresden, Helmholtzstraße 20, 01069 Dresden, Germany*
[2] *Department of Physics, Technical University Dresden, 01069 Dresden, Germany*

(Dated: April 22, 2024)

A range of honeycomb Co oxide compounds has been proposed and investigated in the search for a topological Kitaev spin liquid. Analyzing the quantum chemistry of interacting magnetic moments in $Na_3Co_2SbO_6$, a representative LS-coupled $t_{2g}^5e_g^2$ magnet, we find that the Kitaev and off-diagonal Γ interactions are sizable and antiferromagnetic but still weaker than the Heisenberg contribution. Except Γ', all nearest-neighbor couplings are mainly determined by Coulomb exchange, different from current representations of anisotropic interaction terms. This highlights the limitations of existing anisotropic models and the need for systematic wave-function quantum chemical studies to clarify exchange mechanisms in Kitaev-Heisenberg systems.

Introduction. Mutually orthogonal plaquettes composed of two transition ions (M) and two bridging ligands (L) provide the playground for anisotropic Kitaev magnetic interactions [1]. Such M_2L_2 plaquettes are found in the rocksalt crystal structure and various rhombohedral derivatives: perpendicular to the 111 direction, they form triangular magnetic networks out of which hexagonal configurations can be obtained if certain sites are removed or occupied by nonmagnetic atomic species. While Kitaev physics [1] was initially suggested to occur for LS-coupled t_{2g}^5 transition ions on those types of lattices [2], extensive research is carried out more recently on Co oxide $t_{2g}^5e_g^2$ honeycomb compounds.

Here we nail down the underlying exchange mechanisms in $Na_3Co_2SbO_6$, a honeycomb cobaltate whose macroscopic magnetic properties indicate substantial frustration [3–5], presumably arising from sizable, plaquette-dependent [2, 6–8], anisotropic intersite interactions. We first demonstrate the power of the quantum chemical methodology through a scan of the many-body Co-site multiplet structure, benchmarked against existing inelastic neutron scattering (INS) data [3] and analysis of X-ray spectra [9]. Focusing then on intersite effective couplings, we unveil the morphology of Co-Co anisotropic exchange: the leading nearest-neighbor interaction mechanism is direct, Coulomb exchange according to our quantum chemical study. Direct, Coulomb exchange being completely neglected so far in Kitaev-Heisenberg electronic models, our work redefines the overall map of symmetric anisotropic pseudospin interactions in quantum matter.

Co-site multiplet structure. How the magnetic centers in $Na_3Co_2SbO_6$ should be visualized is detailed in Table I. Here we built on insights gained from quantum chemical investigations of a series of other cobaltates, d^6 [10], d^7 [11], and d^8 [12]. Various features concerning the Co-ion ground state and multiplet structure can be directly compared with info extracted from spectroscopic investigations already carried out on $Na_3Co_2SbO_6$: the degree of $t_{2g}^5e_g^2$–$t_{2g}^4e_g^3$ configurational mixing in the ground-state wave-function [9], the trigonal splitting of the Co $3d$ t_{2g} levels δ [9], and the position of the low-lying '$LS\delta$' exciton [3].

To disentangle crystal-field effects, on-site Coulomb interactions, and spin-orbit couplings (SOCs), quantum chemical calculations (see Supplemental Material, SM, for computational details) were first performed at the single-configuration (SC) $t_{2g}^5e_g^2$ level, i. e., excluding other orbital occupations. This is depicted in the first column of Table I: the Co $3d$ t_{2g} levels are split by trigonal and residual lower-symmetry [13] fields into distinct components. Whether the pair of e levels (or e-like, for symmetry that is even lower than trigonal) is energetically stabilized due to the large pozitive charge within the magnetic plane (formally 5+ Sb ions), similar to e. g. the case of $Cd_2Os_2O_7$ [14], remains to be clarified in a separate study.

By allowing subsequently for all possible orbital occupations within the Co $3d$ shell, which is referred to as complete-active-space self-consistent-field (CASSCF) [15, 16], an admixture of 8% $t_{2g}^4e_g^3$ character is found in the ground-state CASSCF wave-function, in agreement with conclusions drawn from the analysis of X-ray spectra [9]. Interestingly, given the low point-group symmetry [13], the $t_{2g}^5e_g^2$–$t_{2g}^4e_g^3$ interaction implies also Coulomb matrix elements that in cubic environment are 0 by symmetry: the trigonal splitting within the $^4T_{1g}$ manifold is consequently reduced from a bare value of 100 meV (SC results in Table I) to 60 meV (CASSCF data) [17]. Such physics was not discussed so far in effective-model theory [3, 9, 18–20]. Significantly heavier 'dressing' may occur in the case of multi-M-site, molecular-like $j \approx 1/2$ [21] and $j \approx 3/2$ [22] spin-orbit states, up to the point where the picture of 'dressing' even breaks down [22].

Upon including SOCs, at either CASSCF or multireference configuration-interaction (MRCI) [15, 16] level, additional splittings occur. The lowest on-site excitation is computed at 27.5 meV (see footnote f in Table I), in ex-

TABLE I. Co^{2+} $3d^7$ multiplet structure in $Na_3Co_2SbO_6$. SC stands for a single-configuration ($t_{2g}^5 e_g^2$) $S=3/2$ calculation. Each value in the last two columns indicates a Kramers doublet (KD); all $S=3/2$ and 20 (out of 50) $S=1/2$ d^7 states were included in the spin-orbit CASSCF and MRCI computations. Only states with relative energies lower than 2 eV are listed. Notations corresponding to O_h symmetry are used, though the actual point-group symmetry is much lower [13].

Relative energies (eV)	SC	CASSCF[a]	CASSCF[b] +SOC	MRCI +SOC
$^4T_{1g}$ ($t_{2g}^5 e_g^2$)	0	0[c]	0[d]	0
	0.10	0.06	0.03, 0.07 [e]	0.03[f], 0.07
	0.11	0.06	0.13, 0.14, 0.15 [g]	0.13, 0.13, 0.15
$^4T_{2g}$ ($t_{2g}^4 e_g^3$)[h]		0.85	0.81, 0.82	0.88, 0.89
		0.87	0.84, 0.85	0.91, 0.91
		0.88	0.86, 0.88	0.92, 0.94
$^4A_{2g}$ ($t_{2g}^3 e_g^4$)		1.83	1.72, 1.72	1.77, 1.83
^2E_g ($t_{2g}^6 e_g^1$)			1.93, 1.98	1.85, 1.85

[a] Orbitals optimized for the lowest three $S=3/2$ roots; the SC splittings in the adjacent column are obtained using this orbital basis.
[b] Orbitals optimized for all $S=3/2$ and the lowest 20 $S=1/2$ roots.
[c] 8% $t_{2g}^4 e_g^3$ character, as also estimated by van Veenendaal *et al.* [9] from the analysis of X-ray spectra.
[d] 0.33% admixture of excited state configurations through 2nd-order SOCs.
[e] $j=3/2$ multiplet in cubic symmetry.
[f] 27.5 meV, in agreement with the experimentally observed exciton at 28–29 meV [3].
[g] $j=5/2$ multiplet in cubic symmetry.
[h] The $^4T_{1g}$ ($t_{2g}^4 e_g^3$) levels lie at 2.9–3.05 eV.

cellent agreement with the outcome of INS measurements [3]. It is seen that, for the lower part of the spectrum, the MRCI corrections to the CASSCF relative energies are moderate.

Magnetic interactions. Fits of the magnetic excitation spectra of $Na_3Co_2SbO_6$ suggest antiferromagnetic (AF) Kitaev coupling K [3], sizable, AF off-diagonal Γ [3, 5], and that an AF K requires ferromagnetic (FM) Heisenberg interaction with $K \sim |J|$ [4]. A relatively large FM Heisenberg J is also proposed by analysis of effective models relying on Co-Co kinetic exchange, Co-O_2-Co superexchange, and intersite hoppings extracted from density-functional computations [19].

For an *ab initio* quantum chemical perspective, we scanned the nearest-neighbor interaction landscape at the SC (i.e., $t_{2g}^5 e_g^2$–$t_{2g}^5 e_g^2$ Co nearest neighbors, no excited-state configurations considered), CASSCF, and MRCI levels (see SM for details). This allows to distinguish between (i) direct, Coulomb exchange (the only available channel at SC level), (ii) Co-Co kinetic exchange (additionally accounted for in the CASSCF computation with all $3d$ orbitals of the two Co sites considered in the active space), and (iii) Co-O_2-Co superexchange (physics considered by MRCI). Remarkably, for J, K, and Γ, we find that CASSCF and MRCI bring only minor corrections to the SC values (see Table II), indicating that kinetic exchange and superexchange play a marginal role in $Na_3Co_2SbO_6$. This renders the existing exchange models [7, 8, 18–20] obsolete and calls for large-scale quantum chemical studies on Kitaev-Heisenberg magnets.

Also interesting is the effect of on-site excitations, i. e., the admixture of $t_{2g}^4 e_g^3$ character to the leading Co^{2+} $t_{2g}^5 e_g^2$ electron configuration (discussed as well in the previous section), on Γ'. As shown on the second line of Table II, this 'dressing' with virtual on-site excitations reverts the sign of Γ', from FM at the SC level to AF in the SSCAS numerical experiment. The sign of Γ' remains then positive (i. e., AF) when including additional electronic excitations in the CASSCF and MRCI spin-orbit computations (the lowest two lines in Table II).

Transformed to XXZ frame (see the discussion and conversion relations in SM), the nearest-neighbor MRCI coupling parameters change to $J_{xy}=-1.29$, $J_z=-0.44$, $J_{\pm\pm}=-0.20$, and $J_{z\pm}=-0.09$. Their dependence on the various exchange mechanisms is illustrated in Table III: it is seen that J_{xy} is essentially determined by Coulomb

TABLE II. Magnetic couplings (meV) for the C_{2h} Co-Co link [13] in $Na_3Co_2SbO_6$. The lowest singlet, triplet, quintet, and septet associated with each of the possible (3×3) $t_{2g}^5 e_g^2$–$t_{2g}^5 e_g^2$ orbital occupations were included in the spin-orbit treatment, which yields 72 KDs; the lowest four were mapped onto the model of two interacting 1/2 pseudospins, as described in [23, 24]. SSCAS stands for single-site CAS (Co-Co hopping excluded); all possible d-d excitations, on-site + intersite, were considered in CASSCF.

Method	J	K	Γ	Γ'
SC	–1.41	0.45	0.55	–0.16
SSCAS	–1.50	0.57	0.47	0.24
CASSCF	–1.30	0.54	0.50	0.21
MRCI	–1.18	0.53	0.51	0.17

TABLE III. Nearest-neighbor effective magnetic couplings (meV) for the C_{2h} Co-Co link [13] in XXZ representation (see SM or e. g. ref. [19] for conversion relations).

Method	J_{xy}	J_z	$J_{\pm\pm}$	$J_{z\pm}$
SC	–1.34	–1.11	–0.31	0.12
SSCAS	–1.63	–0.68	–0.17	–0.16
CASSCF	–1.43	–0.51	–0.19	–0.12
MRCI	–1.29	–0.44	–0.20	–0.09

exchange, while for the remaining nearest-neighbor effective interactions also other contributions are significant, most of all, the dressing with on-site excitations.

While the discussion has been focussed so far on the pair of edge-sharing CoO_6 octahedra displaying C_{2h} point-group symmetry [13], a similar fine structure is found for the excitation spectrum of the lower-symmetry, C_i Co_2O_{10} unit: the excitation energies of the lowest three excited states (defined by the interaction of the two 1/2 pseudospins) differ on average by 10%. Whether certain details in the experimental spectra can be explained by considering two different sets of Co-Co magnetic links (i. e., two different sets of nearest-, second-, and third-neighbor couplings) remains to be clarified in forthcoming work.

One aspect that deserves elaboration is the possible role of orbital breathing effects [25] in the case of the effective magnetic couplings in $t_{2g}^5e_g^2$ cobaltates since orbital breathing has been found to strongly affect intersite interactions in d^9 copper oxide compounds [25]. In this regard, it is worth to point out that (i) in cuprates, intersite hopping implies changing the occupation of the 'magnetic' x^2-y^2 d orbital (separated energetically by 1 eV or more from the other d components) by 1, from 1 to either 0 or 2; for orbitally degenerate, LS-coupled t_{2g}^5 and $t_{2g}^5e_g^2$ ions, the average magnetic-orbital occupation changes by much less, i. e., by either 0.33 (within the t_{2g} subshell) or 0.5 (within the e_g sector) & (ii) in Cu^{2+} oxides, the relevant M d – L p orbital overlap is σ-type and d-orbital breathing is therefore strongly coupled to M – L – M superexchange physics; for t_{2g}^5 and $t_{2g}^5e_g^2$ species, the relevant M d – L p orbital overlap is π-type and d-orbital breathing (anyhow already much weaker since the modification of the average magnetic-orbital charge is much less dramatic) couples less intensely with superexchange. Those are likely the reasons for which excellent agreement is found between MRCI couplings and experimental effective-coupling estimates in t_{2g}^5 Sr_2IrO_4 [23], which is not the case for MRCI results computed with a minimal CAS kernel in d^9 square-lattice cuprates.

Different from t_{2g}^5 Sr_2IrO_4 and cuprates with corner-sharing ML_4 units, the outcome of experiment-based investigations on $t_{2g}^5e_g^2$ honeycomb cobaltates is less clear-cut. The parameters derived at correlated level in Table II fulfill however the most basic constraints posed by INS [3, 4], neutron diffraction [5], and magnetometry [5] measurements available for $Na_3Co_2SbO_6$: AF K [3], AF Γ [3, 5], and FM J [3, 4]. Reproducing more specific experimental features requires, besides the computed nearest-neighbor interaction parameters and AF second/third-neighbor (J_2/J_3) Heisenberg couplings, cyclic exchange [26–28] and/or farher-neighbor anisotropies, antisymmetric and/or symmetric. Effects of the farther-neighbor symmetric anisotropies are briefly discussed in the following.

The MRCI coupling parameters alone yield a FM ground state on the extended honeycomb lattice. To account for the experimentally observed zigzag-like AF order and the emergence of a structure akin to a 1/3-plateau in the magnetization curves [5], we analyzed the role of longer-range pair interactions, isotropic and with XYZ anisotropy, with the help of exact-diagonalization computations for clusters of 24 sites with periodic boundary conditions (see, e. g., [24] for similar calculations). Mapping the ground-state phase diagram, we found that, in isotropic J_2–J_3 context, AF zigzag order is stabilized for $J_2+J_3 \gtrsim 0.25$ [see Fig.1(a)]. Then, the significant in-plane anisotropy and the 1/3-plateau observed experimentally can be replicated through XYZ longer-range anisotropy: with $J_2^x = 0.10$, $J_2^y = 0.32$, $J_2^z = 0.21$,

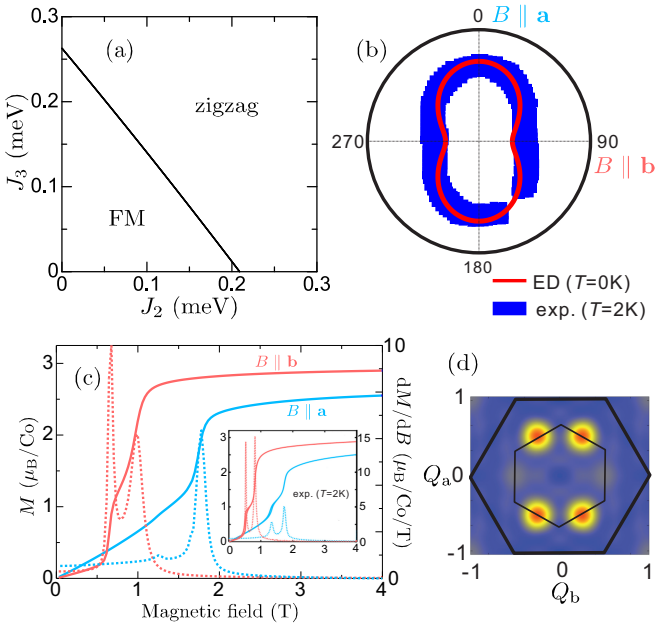

FIG. 1. (a) Ground-state phase diagram in the J_2–J_3 plane using the MRCI values for J, K, Γ, and Γ'. (b) Magnetic susceptibility versus in-plane angle, where 0 and 90 degrees correspond to the **a** and **b** axes, respectively. (c) Magnetization versus magnetic field (solid lines) and its derivative (dashed lines) using $J_2^x = 0.10$, $J_2^y = 0.32$, $J_2^z = 0.21$, $J_3^x = 0.32$, $J_3^y = 0.10$, $J_3^z = 0.21$, and the MRCI nearest-neighbor couplings. Inset: Experimental data extracted from Ref. 5. (d) Static structure factor at $B = 0$.

$J_3^x = 0.32$, $J_3^y = 0.10$, $J_3^z = 0.21$ (meV), $g_a = 5.3$, $g_b = 5.9$, and the nearest-neighbor MRCI couplings, both the angular dependence of the susceptibility and the field dependence of the magnetization curve can be fitted, as illustrated in Figs. 1(b,c). The observed AF wave vectors ($\pm\mathbf{a}^{\prime}/2$, $\pm\mathbf{b}^{\prime}/2$,0) at zero field can also be nicely reproduced. Additional details are provided in SM.

Conclusions. In sum, analyzing the quantum chemistry of interacting magnetic moments in LS-coupled honeycomb cobaltates, we cannot confirm kinetic exchange and superexchange as leading mechanisms for anisotropic intersite effective couplings. Instead, our *ab initio* computations reveal Coulomb exchange as main player, an ingredient not considered so far in existing models [2, 6–8, 18–20]. As co-mechanism to intersite interactions, both isotropic and anisotropic, it has already been pointed out in quantum chemical studies on hexagonal d^5 $RuCl_3$ [29], triangular-lattice d^5 $NaRuO_2$ [29, 30], square-lattice d^5 Ba_2IrO_4 [31], square-lattice d^9 cuprates [32, 33], and d^9 cuprate chains [34]; spotting it as driving force in hexagonal d^7 cobaltates portrays in even sharper tones the shortcomings of present Kitaev-Heisenberg exchange models. In light of the quantum chemical findings, effective-model electronic-structure investigations ignoring Coulomb exchange cannot provide meaningful predictions on material trends, be it bulk or heterostructures. Our analysis additionally signalizes the possible role of farther neighbor exchange anisotropies. The latter may account for the 1/3-plateau observed experimentally in the magnetization curves [5].

Acknowledgments. We thank A. Tsirlin, R. C. Morrow, and S. L. Drechsler for discussions and U. Nitzsche for technical support. P. B., T. P., and L. H. acknowledge financial support from the German Research Foundation (Deutsche Forschungsgemeinschaft, DFG), project number 468093414. S. N. acknowledges financial support through the SFB 1143 of the DFG.

[1] A. Kitaev, Ann. Phys. **321**, 2 (2006).
[2] G. Jackeli and G. Khaliullin, Phys. Rev. Lett. **102**, 017205 (2009).
[3] C. Kim, J. Jeong, G. Lin, P. Park, T. Masuda, S. Asai, S. Itoh, H.-S. Kim, H. Zhou, J. Ma, and J.-G. Park, J. Phys. Condens. Matter **34**, 045802 (2021).
[4] A. L. Sanders, R. A. Mole, J. Liu, A. J. Brown, D. Yu, C. D. Ling, and S. Rachel, Phys. Rev. B **106**, 014413 (2022).
[5] X. Li, Y. Gu, Y. Chen, V. O. Garlea, K. Iida, K. Kamazawa, Y. Li, G. Deng, Q. Xiao, X. Zheng, Z. Ye, Y. Peng, I. A. Zaliznyak, J. M. Tranquada, and Y. Li, Phys. Rev. X **12**, 041024 (2022).
[6] G. Khaliullin, Prog. Theor. Phys. Supp. **160**, 155 (2005).
[7] H. Liu and G. Khaliullin, Phys. Rev. B **97**, 014407 (2018).
[8] R. Sano, Y. Kato, and Y. Motome, Phys. Rev. B **97**, 014408 (2018).
[9] M. van Veenendaal, E. H. T. Poldi, L. S. I. Veiga, P. Bencok, G. Fabbris, R. Tartaglia, J. L. McChesney, J. W. Freeland, R. J. Hemley, H. Zheng, J. F. Mitchell, J.-Q. Yan, and D. Haskel, Phys. Rev. B **107**, 214443 (2023).
[10] L. Hozoi, U. Birkenheuer, H. Stoll, and P. Fulde, New J. Phys. **11**, 023023 (2009).
[11] M. Iakovleva, T. Petersen, A. Alfonsov, Y. Skourski, H.-J. Grafe, E. Vavilova, R. Nath, L. Hozoi, and V. Kataev, Phys. Rev. Mater. **6**, 094413 (2022).
[12] C. Albert, T. J. Ballé, F. A. Breitner, Y. Krupskaya, A. Alfonsov, Z. Zangeneh, S. Avdoshenko, M. S. Eldeeb, L. Hozoi, A. Vilangottunjalil, E. Haubold, A. Charnukha, B. Büchner, A. Jesche, and V. Kataev, Inorg. Chem. **60**, 4497 (2021).
[13] L. Viciu, Q. Huang, E. Morosan, H. Zandbergen, N. Greenbaum, T. McQueen, and R. Cava, J. Solid State Chem. **180**, 1060 (2007).
[14] N. A. Bogdanov, R. Maurice, I. Rousochatzakis, J. van den Brink, and L. Hozoi, Phys. Rev. Lett. **110**, 127206 (2013).
[15] T. Helgaker, P. Jørgensen, and J. Olsen, *Molecular Electronic Structure Theory* (John Wiley & Sons, Chichester, 2000).
[16] D. A. Kreplin, P. J. Knowles, and H.-J. Werner, J. Chem. Phys. **152**, 074102 (2020).
[17] While ${}^4T_{1g}(t_{2g}^5 e_g^2)$–${}^4T_{1g}(t_{2g}^4 e_g^3)$ interaction occurs already in cubic environment, differential effects may appear within the group of 'initial' T_{1g} levels in symmetry lower than O_h.
[18] H. Liu, J. Chaloupka, and G. Khaliullin, Phys. Rev. Lett. **125**, 047201 (2020).
[19] S. M. Winter, J. Phys. Mater. **5**, 045003 (2022).
[20] X. Liu and H.-Y. Kee, Phys. Rev. B **107**, 054420 (2023).
[21] T. Petersen, L. Prodan, K. Geirhos, H. Nakamura, I. Kézsmárki, and L. Hozoi, Sci. Rep. **13**, 2411 (2023).
[22] T. Petersen, P. Bhattacharyya, U. K. Rößler, and L. Hozoi, Nat. Commun. **14**, 5218 (2023).
[23] N. A. Bogdanov, V. M. Katukuri, J. Romhányi, V. Yushankhai, V. Kataev, B. Büchner, J. van den Brink, and L. Hozoi, Nat. Commun. **6**, 7306 (2015).
[24] R. Yadav, N. A. Bogdanov, V. M. Katukuri, S. Nishimoto, J. van den Brink, and L. Hozoi, Sci. Rep. **6**, 37925 (2016).
[25] N. A. Bogdanov, G. L. Manni, S. Sharma, O. Gunnarsson, and A. Alavi, Nat. Phys. **18**, 190 (2022).
[26] W. G. F. Krüger, W. Chen, X. Jin, Y. Li, and L. Janssen, Phys. Rev. Lett. **131**, 146702 (2023).
[27] N. Francini and L. Janssen, Phys. Rev. B **109**, 075104 (2024).
[28] Y. Gu, X. Li, Y. Chen, K. Iida, A. Nakao, K. Munakata, V. O. Garlea, Y. Li, G. Deng, I. A. Zaliznyak, J. M. Tranquada, and Y. Li, Phys. Rev. B **109**, L060410 (2024).
[29] P. Bhattacharyya, T. Petersen, N. A. Bogdanov, and L. Hozoi, Commun. Phys. **7**, 121 (2024).
[30] P. Bhattacharyya, N. A. Bogdanov, S. Nishimoto, S. D. Wilson, and L. Hozoi, npj Quantum Mater. **8**, 52 (2023).
[31] V. M. Katukuri, V. Yushankhai, L. Siurakshina, J. van den Brink, L. Hozoi, and I. Rousochatzakis, Phys. Rev. X **4**, 021051 (2014).
[32] R. L. Martin, J. Chem. Phys. **98**, 8691 (1993).
[33] A. van Oosten, R. Broer, and W. Nieuwpoort, Chem. Phys. Lett. **257**, 207 (1996).
[34] M. Matsuda, J. Ma, V. O. Garlea, T. Ito, H. Yamaguchi,

K. Oka, S.-L. Drechsler, R. Yadav, L. Hozoi, H. Rosner, R. Schumann, R. O. Kuzian, and S. Nishimoto, Phys. Rev. B **100**, 104415 (2019).